

REVISTA DE METALURGIA, 46 (1)
ENERO-FEBRERO, 22-36, 2010
ISSN: 0034-8570
eISSN: 1988-4222
doi: 10.3989/revmetalm.0852

Some kinetics aspects of chlorine-solids reactions^(*)

N. Kanari*, D. Mishra**, J. Mochón***, L.F. Verdeja****, F. Diot* and E. Allain*

Abstract

The present paper describes detailed kinetics investigations on some selected chlorine-solid reactions through thermogravimetric measurements. The solids studied in this article include chemical pure oxides and sulfides as well as their natural bearing materials. The chlorinating agents employed are gaseous mixtures of Cl_2+N_2 (chlorination), Cl_2+O_2 (oxychlorination), and Cl_2+CO (carboclorination). Results are presented as effects of various parameters on the reaction rate of these solids with these chlorinating agents. It was observed that the reactivity of these solids towards different chlorinating agents varied widely. Sulfides could be chlorinated at room temperature, while carboclorination of chromium (III) oxide was possible only above 500 °C. The variation of the chlorination rate of these complex materials with respect to gas velocity, composition and temperature enabled us to focus some light on the plausible reaction mechanisms and stoichiometries. The obtained results were used for selective removal of iron from chromite concentrates, extraction of valuable metals from sulfide materials, purification of MgO samples, etc.

Keywords

Thermogravimetric analysis; Complex oxides; Sulfides; Chlorination; Oxychlorination; Carboclorination; Kinetics.

Algunos aspectos cinéticos de las reacciones de sólidos con cloro

Resumen

Este trabajo describe detalladas investigaciones cinéticas en algunas reacciones seleccionadas de cloro-sólido a través de medidas termogravimétricas. Los sólidos estudiados en este artículo incluyen óxidos químicos puros y sulfuros, así como sus materiales naturales de soporte. Los agentes de cloración empleados son mezclas de gases de Cl_2+N_2 (cloración), Cl_2+O_2 (oxiclорación) y Cl_2+CO (carbocloración). Los resultados se presentan como efecto de varios parámetros en el porcentaje de reacción de estos sólidos con los agentes de cloración. Se ha observado que la reactividad de estos sólidos a través de diferentes agentes de cloración varía ampliamente. Los sulfuros se pudieron clorar a temperatura ambiente mientras que la carbocloración del óxido de cromo (III) sólo fue posible por encima de los 500 °C. La variación del porcentaje de cloración de estos materiales complejos con respecto a la velocidad del gas, composición y temperatura permitió arrojar alguna luz en los posibles mecanismos de reacción y estequiometrías. Los resultados obtenidos se han usado para la eliminación selectiva del hierro de concentrados de cromo, extracción de metales valiosos de materiales sulfhídricos, purificación de muestras de MgO, etc.

Palabras clave

Análisis termogravimétrico; Óxidos complejos; sulfuros; Cloración; Oxiclорación; Carbocloración; Cinética.

1. INTRODUCTION

It is well known that chlorine possesses a high reactivity towards different substances at low temperatures. Further, many metal chlorides and/or oxychlorides have low boiling points and also have appreciably different vapor pressures at a particular temperature. These aspects led the “chlorine

technique” as the subject of much attention in areas like mineral beneficiation, metal extraction and waste treatment. Many important articles devoted to the chlorination can be found in the literature^[1]. The present paper mainly focuses on the kinetics aspects of chlorine-solids reactions approached through thermogravimetric measurements. Besides, higher selectivity of the chlorination methods by

^(*) Trabajo recibido el día 4 de diciembre de 2008 y aceptado en su forma final el día 3 de julio de 2009.

* Laboratoire Environnement et Minéralurgie, UMR 7569 CNRS, Nancy-University, ENSG, BP 40, 54501 Vandoeuvre-lès-Nancy Cedex, France. e-mail: ndue.kanari@ensg.inpl-nancy.fr

** National Metallurgical Laboratory (NML), Jamshedpur, India – 831 007.

*** CENIM - CSIC, Av. Gregorio del Amo 8. Madrid 28040, Spain.

**** E.T.S.I. de Minas de Oviedo, Cátedra de Siderurgia, Independencia s/n. Oviedo 33004, Spain.

employing different chlorinating medium such as oxychlorination ($\text{Cl}_2 + \text{O}_2$) or carbochlorination ($\text{Cl}_2 + \text{CO}$) is also discussed. Below paragraphs depict some examples where detailed kinetic studies were made.

The first example presents how Cl_2 can be used at low temperature for extraction of non-ferrous metals from sulfide concentrates (CuFeS_2 , PbS , ZnS , FeS_2 , etc.). It was observed that these sulfides interact with chlorine even at room temperature^[2-4]. At about 300 °C, generated iron and sulfur chlorides were volatilized whilst the valuable metal chlorides (CuCl_2 , PbCl_2 , and ZnCl_2) were essentially concentrated in the chlorination residues. More than 95 % of copper contained in the concentrate was recovered in the residue at 300 °C as water soluble CuCl_2 .

The second case study presented is the upgrade of lean chromite ores and/or concentrate. It may be mentioned that, physical beneficiation of this material is almost impossible. Chlorination of chromite was carried out in presence of a reducing agent (for example CO). Results obtained earlier^[2, 5] indicated that the carbochlorination ($\text{Cl}_2 + \text{CO}$) of this material at about 550 °C led to preferential extraction of iron. The chlorination extent of chromium was negligible and the Cr/Fe ratio was almost doubled in the residues, compared with that of the raw sample. Carbochlorination at higher temperatures led to a total extraction of chromite elements as chlorides (CrCl_3 , FeCl_3 , AlCl_3 , and MgCl_2). A selective condensation of the gaseous phase allowed the recovery of almost pure MgCl_2 . Similarly, the chromium chloride was separated from those of iron and aluminum.

The third example presents the selectivity of chlorination reaction in the presence of oxygen. This approach was used for the selective chlorination of elements contained in the chromite^[2, 6, 7] and for purification of magnesium oxide through selective chlorination and removal of iron oxides^[8].

In order to have better understanding of the chlorination (Cl_2), carbochlorination ($\text{Cl}_2 + \text{CO}$) and oxychlorination ($\text{Cl}_2 + \text{O}_2$) behavior of various raw materials, and detailed kinetic studies of these solids with various chlorinating gas mixtures were undertaken. The main objective of this article is to demonstrate the usefulness of simple thermogravimetric analyses (TGA) methods for effective measurement of chlorination kinetics of above mentioned selected solid samples with various chlorinating gas mixtures. The obtained kinetic information can be subsequently used for the upgrade of lean ores, such as chromites, complex sulfides, etc., and/or extraction of several valuable metals such as Cu, Mg, Pb etc.

2. METHODOLOGY OF THE KINETICS STUDY

The methodology adopted for the kinetics studies of various solid samples with different chlorinating gaseous mixtures consists in the following:

1. thermogravimetric analysis (TGA) using non-isothermal conditions,
2. batch-boat experiments and analysis of the solid products (SEM, microprobe, XRD, chemical analysis, etc.),
3. comparison of the reaction rate with that of volatilization of the reaction products,
4. determination of adequate gaseous mixture flow rate,
5. effect of the reactive gases proportions on the reaction rate,
6. determination of the apparent reaction orders with respect to the reactive gases,
7. evaluation of the apparent activation energy of the reaction (effect of temperature),
8. mathematical data processing in order to define the geometry of the reaction interface
9. indication of the possible rate controlling step.

Detailed results of the chlorination kinetics of different solids were reported in literature^[2-10]. Only some typical examples will be described illustrating the stages of these kinetics studies. The materials and experimental procedure are briefly depicted in the next section. However, more accurate conditions for each kinetics example will be given during the development of each individual kinetic study.

3. MATERIALS AND EXPERIMENTAL PROCEDURE

The sulfides' samples used in this investigation were the chalcopyrite (CuFeS_2), pyrite (FeS_2), galena (PbS) and sphalerite (ZnS). The elemental and mineralogical compositions of these samples of natural origin were determined by Scanning Electron Microscopy (SEM) and X-ray diffraction (XRD) analyses. Besides, a high grade copper concentrate "HGCC" was also used. It contains about 81.7 % CuFeS_2 , 6.4 % ZnS , 5.7 % lead compounds, 3.0 % iron sulfides and less than 1.0 % SiO_2 . The oxides' samples of chromium (Cr_2O_3), iron (Fe_2O_3) and magnesium (MgO) were supplied by PROLABO (Paris, France). They are of synthetic origin and have a purity as high as 99 %. The chromite sample used for this study was obtained from a chromite concentrate by successive separations in dense liquor in order to separate the gangue from the chromite

mineral. Results of the microprobe and classical chemical analysis suggest that the chromite sample could be represented as: $(\text{Fe}^{2+}_{0.30}, \text{Mg}_{0.70})(\text{Cr}_{1.56}, \text{Al}_{0.37}, \text{Fe}^{3+}_{0.07})\text{O}_4$. All used samples were in powder state with low specific surface areas indicating a week grains' porosity.

The thermogravimetric analysis (TGA) were performed using a micro-electronic balance CAHN type C 1000. The accuracy of this type of apparatus is about 0.1 % for a sensitivity of 0.5 μg . The (Cl_2 , CO , O_2 , N_2) gas flows are measured separately. They can be mixed and homogenized. Almost all the residual moisture of these gases is eliminated by circulation through CaCl_2 columns. The gas inlet system is built so that the gases are preheated before reacting with the sample. The temperature and the weight of the sample are recorded continuously as a function of time by a data acquisition system.

The thermogravimetric analysis is run using continuous temperature raise or isotherm modes. The experimental protocol was the following:

1. an amount of sample of about 40 mg was scattered uniformly in a large quartz nacelle,
2. during the non isothermal treatment, the pure gases or gas mixtures (Cl_2 , CO , Cl_2+N_2 , Cl_2+CO , $\text{Cl}_2+\text{CO}+\text{N}_2$, Cl_2+O_2 and/or $\text{Cl}_2+\text{O}_2+\text{N}_2$) were flown through the reactor and at the same time the furnace power was switched on,
3. for the isotherm mode experiment the sample was preheated in a low nitrogen flow up to the desired temperature, this before flowing the reactive gases through the reactor,
4. at the end of the predetermined treatment time, the reactive gases were replaced by nitrogen and the furnace is lowered down, and the reactor cools down as a result of N_2 flow,
5. the nacelle was taken out from the reactor and weighted. The treatment product was set aside for different analyses.

Few batch-boat chlorination tests were also performed in a horizontal experimental set-up. This set-up was composed of a gas metering unit followed by a gas purification system and a horizontal furnace. The gaseous reaction products were recovered through condensers and the outlet gases were purified before their release to the atmosphere. The reaction products (chlorination residues as well as condensates) were examined by SEM, XRD and chemical analyses.

Data obtained from different treatments were initially plotted as evolution of % weight change as a function of time. All negative values represent % weight losses (% WL), whilst positive ones express the % weight gains.

4. RESULTS AND DISCUSSION

4.1. Thermogravimetric analysis using non-isothermal conditions

These experiments could give preliminary information on the temperature range for the kinetic studies. In other words, TGA allows rapidly the evaluation of the reactivity of various solids towards chlorinating gas mixtures. For example, in figure 1 the percentage weight change of several sulfides with respect to temperature during their chlorination with Cl_2+N_2 gas mixture under non-isothermal conditions with a heating rate (dT/dt) of about $20\text{ }^\circ\text{C}/\text{min}$ are presented.

Several important information are obtained from this figure such as: chalcopyrite starts to react with chlorine even at room temperature, at higher temperature this reaction leads to the formation of cupric, ferric, and sulfur chlorides as final reaction products^[2]; for pyrite initial weight gain was observed due to the substitution of sulfur by chlorine, while the weight losses of this sample at temperature higher than $250\text{ }^\circ\text{C}$ were attributed to the volatilization of ferric chloride; sphalerite and the galena started to react with chlorine at temperatures higher than $200\text{ }^\circ\text{C}$ generating their respective chlorides. Full reaction and volatilization of the chlorination products of the studied sulfides took place at higher temperatures.

However, the chlorination of sulfides is very complex and is difficult to be explained only by their treatment in non isothermal conditions. In order to have an insight about the pure sulfides' chlorination, a series of batch-boat tests was performed between room temperature and $750\text{ }^\circ\text{C}$ for a reaction time of 2 h. Results were drawn as

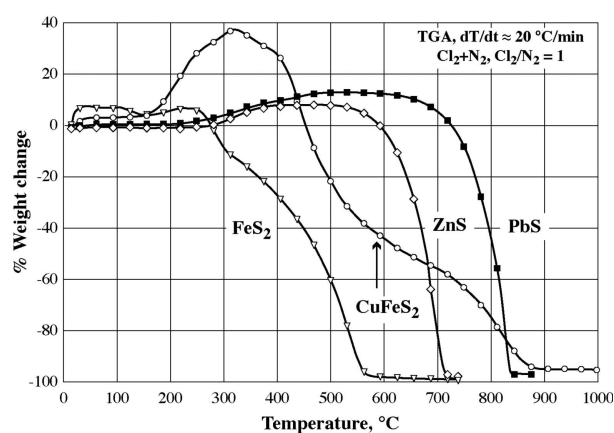


Figure 1. TGA of several sulfides in Cl_2+N_2 .

Figura 1. ATG de algunos sulfuros en atmósfera de Cl_2+N_2 .

evolution of weight change as function of the temperature in figure 2. A high grade copper concentrate "HGCC" composed essentially of chalcopirite was also treated in same conditions. The chlorination residues and condensates were systematically analyzed by SEM and XRD analysis. The chlorination residues of HGCC were subjected to chemical analysis for copper and iron contents.

The presence of chlorine, as observed by SEM, in the chlorination residue obtained at room temperature for CuFeS_2 , FeS_2 and HGCC indicates that chlorine had reacted with these sulfides. The peak intensity of sulfur decreased with the temperature rise, while that of chlorine increased. At 300 °C, SEM analysis showed that the residues obtained from chlorination CuFeS_2 and HGCC were sulfur-free indicating that full chlorination of the sulfides was achieved. XRD results showed the presence of CuCl_2 , besides non reacted CuFeS_2 , in the chlorination residue of chalcopirite and HGCC samples from room temperature.

Condensates of chlorination of FeS_2 , CuFeS_2 and HGCC were significantly observed at temperatures higher than 200 °C. These condensates were essentially

composed of Fe and Cl for a chlorination temperature lower than 300 °C showing that iron was removed as FeCl_3 which is characterized by a vapor pressure of about 1 atm at temperatures close to 300 °C (Fig. 3). At temperatures equal and higher than 400 °C, copper

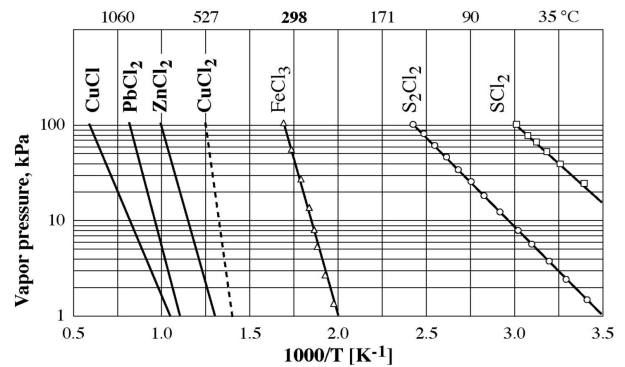
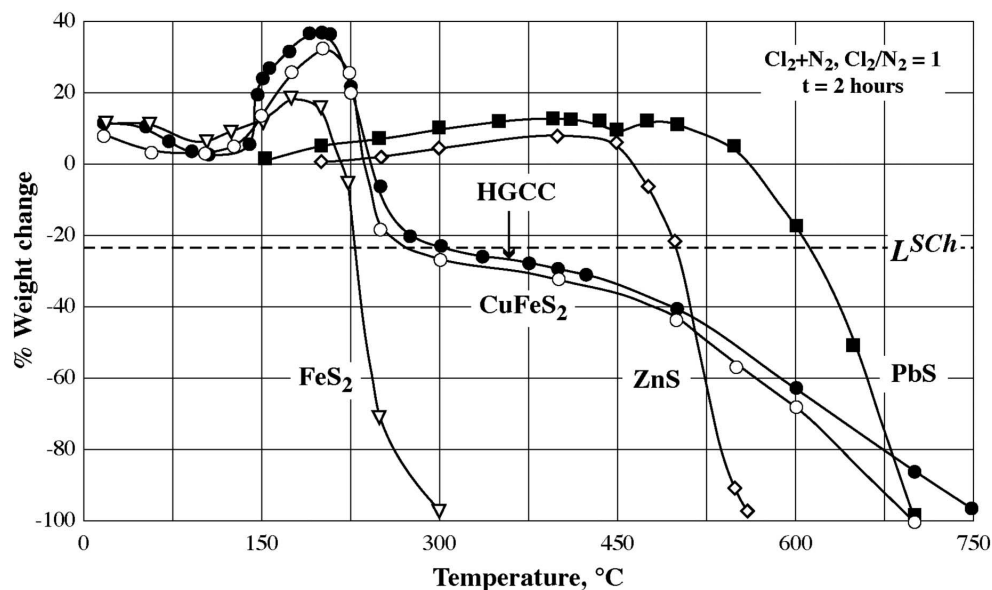


Figure 3. Evolution of vapor pressure of several chlorides versus inverse of temperature.

Figura 3. Evolución de la presión de vapor de algunos cloruros frente al inverso de la temperatura.



L^{Sch} : Theoretical limit for de selective chlorination of HGCC (high grade copper concentrate) supposing full chlorination of sulphides and volatilization of iron and sulphur chlorinated.

L^{Sch} : Límite teórico de la cloruración selectiva de un concentrado de calcopirita con alto contenido en cobre (HGCC) suponiendo una completa cloración de los sulfuros presentes y la volatilización de compuestos sulfurados de hierro y de otros elementos metálicos (FeS_2 , ZnS y PbS) que han reaccionado con el cloro.

Figure 2. Evolution of % weight change versus temperature during chlorination of several sulfides and a high grade copper concentrate 'HGCC' in Cl_2+N_2 for 2 h.

Figura 2. Evolución del % de cambio de peso frente a la temperatura durante la cloración de varios sulfuros y un concentrado de cobre con un alto contenido de cobre en atmósfera de Cl_2+N_2 durante 2 h.

was also detected in the condensate of CuFeS_2 and HGCC chlorination. Sulfur was not detected in the solid condensates regardless of the chlorination temperature, indicating that sulfur was essentially removed as S_xCl_y ($\text{S}_2\text{Cl}_2 + \text{SCl}_2$ and intermediates) which have sufficiently high vapor pressures (Fig. 3) to be transported out by the exhaust gases. The formation of sulfur dichloride is probably due to high partial pressure of chlorine in the chlorination process. The formation of cuprous chloride (CuCl) during chlorination of CuFeS_2 and HGCC was confirmed by XRD at temperature equal or higher than 600°C . It is probably product of cupric chloride decomposition in spite of high partial pressure of chlorine.

The qualitative analyses such as SEM and XRD indicated that, in our conditions, the temperatures close to 300°C were adequate for the full chlorination of pyrite and chalcopyrite and for the volatilization of sulfur and iron chlorinated compounds. The chemical analysis of chlorination residue of HGCC showed that complete iron extraction was achieved at 300°C and all copper is concentrated in the residue. The theoretical limit of selective chlorination of HGCC (L^{Sch} in figure 2) is fully consistent with % WL of sample and extraction extent of iron obtained at 300°C . The copper extraction started at higher and about 40 pct of copper were extracted at 600°C .

The sulfides of zinc and lead reacted with chlorine at temperatures equal to or higher than 150°C leading to their respective chlorides. However, complete reaction of ZnS was achieved at temperature lower than that of PbS . The chlorination of these sulfides is also complicated by the formation of liquid phases (M.p. of ZnCl_2 is 283°C) and/or formation of an eutectic at 450°C in the PbS-PbCl_2 system.

The complete chlorination of the selected sulfides can be classified by following descending order $\text{FeS}_2 > \text{CuFeS}_2 > \text{ZnS} > \text{PbS}$. It seems that this sequence follows the evolution of vapor pressure of chlorides as shown by figure 3. Nevertheless, other phenomena could occur during chlorination of sulfide at high temperatures such as decomposition of chalcopyrite and pyrite to cubanite and pyrrotite, respectively and/or volatilization of lead sulfide.

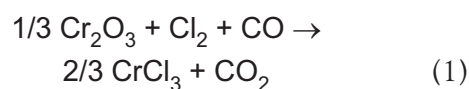
Pertinently to these results, the chlorination kinetics of these sulfides at temperature $\leq 300^\circ\text{C}$ were studied in details in former works^[2-4].

4.2. Comparison of the reaction rate with that of volatilization of the reaction products

The reactions of chlorine with a solid generate chlorides which have particular vapor pressure at a

given temperature. Consequently, temperature plays a crucial role in kinetic measurements, which defines the proportion of chlorides that volatilized to that of which remains in the reaction zone (unvolatilized). Use of TGA technique to measure the evolution of the reaction extent require that either the volatilization rate of the reaction products is higher than that of its rate of formation or the chlorinated products remain completely in the reaction zone under the studied temperature range.

Figure 4 illustrates an example of Cr_2O_3 carbochlorination using non-isothermal^[2-10]. The reaction of Cr_2O_3 with $\text{Cl}_2 + \text{CO}$ can be described by equation (1).



Assuming that chromium (III) chloride (CrCl_3) is the only chlorinated product of the reaction, the volatilization of CrCl_3 was tested in the same gaseous mixture ($\text{Cl}_2 + \text{CO}$). Results are also depicted in figure 4. It is clear from this figure, that the rate of volatilization of CrCl_3 at temperatures above 500°C is higher than its rate of formation through the reaction of Cr_2O_3 with $\text{Cl}_2 + \text{CO}$. In these conditions, the observed weight loss of Cr_2O_3 reaction with $\text{Cl}_2 + \text{CO}$ could be a direct measure of the extent of Cr_2O_3 carbochlorination reaction.

The chlorination of the magnesium oxide represents another case study. The reaction of MgO with chlorine (Eq. (2)), in absence of a reducing atmosphere, takes

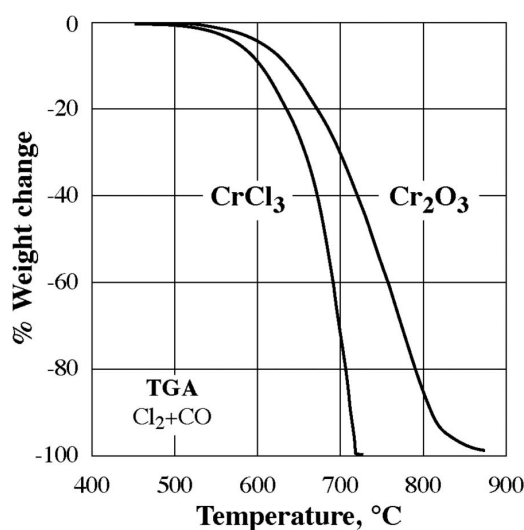
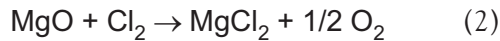


Figure 4. TGA of Cr_2O_3 and CrCl_3 in $\text{Cl}_2 + \text{CO}$.

Figura 4. ATG del Cr_2O_3 y CrCl_3 en atmósfera de $\text{Cl}_2 + \text{CO}$.

place at $T > 600\text{ }^{\circ}\text{C}$ [2-10]. Magnesium chloride has melting and boiling points of $714\text{ }^{\circ}\text{C}$ and $1,412\text{ }^{\circ}\text{C}$, respectively. One possible way to decrease the reaction rate of MgO with chlorine is to increase the partial pressure of oxygen in the system. This can lead to a volatilization rate of MgCl_2 , obtained according equation (2), higher than that of its formation.



A series of MgO chlorination tests was performed at $950\text{ }^{\circ}\text{C}$, using a $\text{Cl}_2 + \text{O}_2$ gas mixture with an oxygen content that varied from 0 to 66.7 % (molar %). Figure 5 shows the evolution of % weight change of MgO sample versus time during its oxychlorination for the conditions mentioned above. This figure suggests that the chlorinating gas mixtures containing more than 90 % of Cl_2 lead to a chlorination rate that is higher than that of MgCl_2 volatilization. For this reason, the kinetics of MgO oxychlorination was studied using a $\text{Cl}_2 + \text{O}_2$ gas mixture containing a chlorine content less than or equal to 80 % [8]. Then, the carbochlorination kinetics of MgO in $\text{Cl}_2 + \text{CO}$ was investigated at temperatures lower than the melting point of MgCl_2 [10] assuming that the MgCl_2 volatilization is negligible.

4.3. Determination of adequate gaseous mixture velocity

In order to determine the intrinsic parameters of the gas-solid reaction, it is necessary to minimize the effect of external mass transfer phenomena. This can be

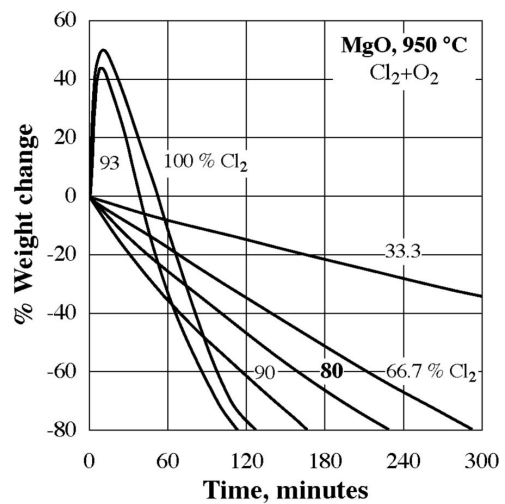


Figure 5. Evolution of % weight change as function of time during isothermal treatment of MgO in $\text{Cl}_2 + \text{O}_2$ at various chlorine contents.

Figura 5. Evolución del % de cambio de peso como función del tiempo durante el tratamiento isotérmico de MgO en atmósfera de $\text{Cl}_2 + \text{O}_2$ con diferentes contenidos de cloro.

achieved by using a high velocity of reactive gases such that the reaction rate becomes unaffected. As the mass transfer phenomena are promoted at high temperature, the effect of the gas velocity on the reaction rate of a chlorination reaction was studied at high temperature [2] or at two different temperatures. The experimental results of the effect of $\text{Cl}_2 + \text{O}_2$ velocity on the oxychlorination of Fe_2O_3 at $750\text{ }^{\circ}\text{C}$ and $950\text{ }^{\circ}\text{C}$ are given in figure 6. They indicate that the gas velocities

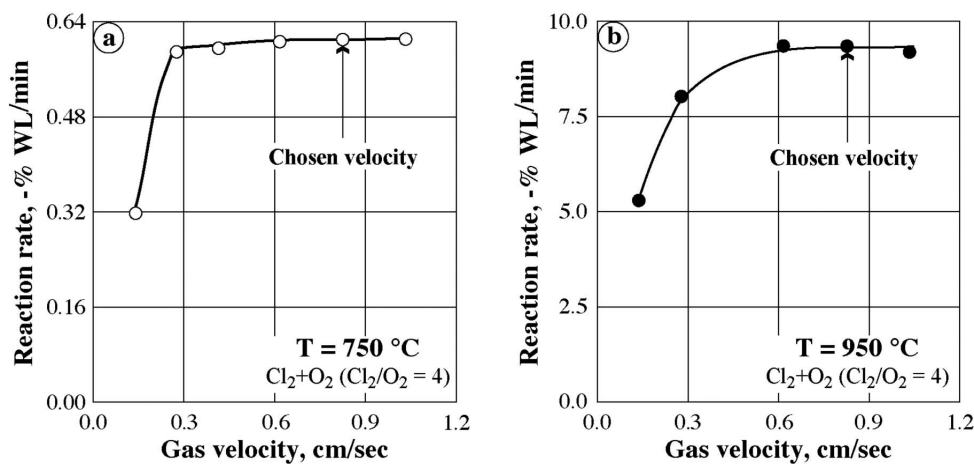


Figure 6. Oxychlorination rate of Fe_2O_3 versus gas velocity of $\text{Cl}_2 + \text{O}_2$ at (a) $750\text{ }^{\circ}\text{C}$ and (b) $950\text{ }^{\circ}\text{C}$.

Figura 6. Tasa de la volatilización por oxicloraación del Fe_2O_3 en relación a la velocidad de un fluido gaseoso de $\text{Cl}_2 + \text{O}_2$ (a) $750\text{ }^{\circ}\text{C}$ y (b) $950\text{ }^{\circ}\text{C}$.

higher than 0.6 cm/second are sufficient to minimize the effect of external mass transfer at both chosen temperatures. Consequently, all kinetic parameters of hematite oxychlorination were investigated by using a gases velocity of about 0.83 cm/s.

4.4. Effect of the reactive gases composition on the reaction rate

The gaseous mixtures used in the chlorination studies were Cl_2+CO , Cl_2 , and Cl_2+O_2 . As it could be expected, the rate of a chlorination reaction will be

affected by the ratio of these gases in the chosen gaseous mixture.

The following examples demonstrate the effects of the Cl_2/CO and Cl_2/O_2 ratios on the chlorination reaction rates of several oxides. Experimental results are summarized in figure 7. The results of carbochlorination rate of Cr_2O_3 at 800 °C, as a function of $\text{Cl}_2/(\text{Cl}_2+\text{CO})$ molar ratio is shown in figure 7 a). The reaction rate of Cr_2O_3 with 100 % CO is almost equal to zero and rises when the chlorine content in the gas mixture increases. It reaches a maximum value for a $\text{Cl}_2/(\text{Cl}_2+\text{CO})$ ratio of ≈ 0.5 . Beyond this ratio, the reaction rate decreases as the chlorine content increases and reaches a minimum

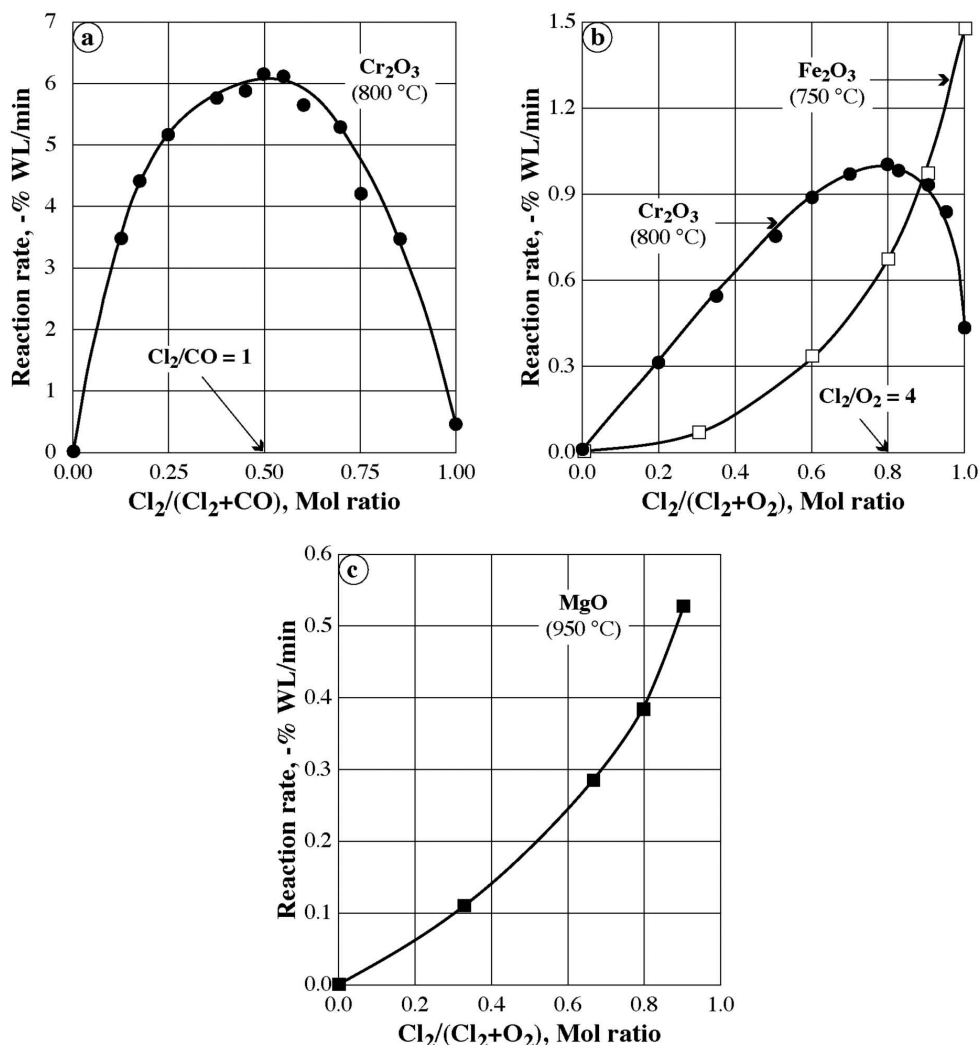
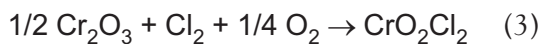


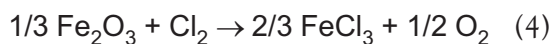
Figure 7. Evolution of the reaction rates as a function of the reactive gases ratios for: (a) carbochlorination of Cr_2O_3 at 800 °C; (b) oxychlorination of Cr_2O_3 at 800 °C and Fe_2O_3 at 750 °C and (c) oxychlorination of MgO at 950 °C.

Figura 7. Evolución de las tasas de reacción en función de cocientes de reacción de los gases para: (a) carbochloración de Cr_2O_3 a 800 °C; (b) oxicloraación de Cr_2O_3 a 800 °C y Fe_2O_3 a 750 °C y (c) oxicloraación de MgO a 950 °C.

value with 100 % Cl₂. The observed maximum reaction rate at Cl₂/(Cl₂+CO) ratio of 0.5 suggests that the carbochlorination of Cr₂O₃ with Cl₂+CO follows equation (1). The effect of the Cl₂/(Cl₂+O₂) molar ratio on the oxychlorination of Cr₂O₃ at 800 °C is represented in figure 7 b). The oxychlorination rates passes by a maximum corresponding to a Cl₂/(Cl₂+O₂) molar ratio of about 0.8. This value corresponds to a molar ratio of Cl₂/O₂ equal to 4. These results show that chlorination of Cr₂O₃ with Cl₂+O₂ gas mixture takes place according to equation (3) involving the formation of chromium oxychloride as the main reaction product.



As this could be expected, the oxychlorination rate of Fe₂O₃ (Fig. 7 b)) increases when the Cl₂/(Cl₂+O₂) molar ratio augments and it reaches a maximum value for the chlorination in absence of oxygen. Thus chlorination of Fe₂O₃ can be described by equation (4).



Similarly, the reaction rate of MgO with Cl₂+O₂ (Fig. 7 c)) augments with the decrease of oxygen content in the Cl₂+O₂ gas mixture. This may be explained by the fact that the presence of oxygen in the gas mixture will shift the reaction of equation (2) to the left side.

4.5. The apparent reaction orders with respect to the reactive gases

4.5.1. Apparent reaction orders with respect to Cl₂ and O₂

To determine the apparent reaction order with respect to Cl₂, a series of experimental tests were carried out at constant partial pressure of oxygen (0.33 atm) and the chlorine partial pressure was varied in a defined interval. Similarly, the apparent reaction order with respect to O₂ was derived from the experimental results at constant Cl₂ partial pressure (0.33 atm). In all cases, the chosen gas velocities correspond to optimal values defined previously. Nitrogen was used as a carrier gas.

4.5.2. Apparent reaction order with respect to Cl₂+O₂

A gas mixture of Cl₂+O₂+N₂ with a velocity of 0.55 cm/second was used. The Cl₂/O₂ molar ratio of the

gas mixture was kept constant at 4, while the partial pressure of Cl₂+O₂ was varied from 0.38 to 1.00 atm.

As indicated by figure 8, the apparent reaction orders for Cr₂O₃ oxychlorination at 800 °C with respect to Cl₂, O₂, and Cl₂+O₂ are respectively about 1.08, 0.23 and 1.29. One may note that the presence of oxygen enhances the reaction rate since ⁿO₂ = 0.23. This observation agrees well with the oxychlorination of Cr₂O₃ (Eq. (3)) that consumes oxygen to generate chromium (VI) oxychloride (CrO₂Cl₂).

As a contrast, the apparent reaction order with respect to Cl₂, O₂, and Cl₂+O₂ for MgO oxychlorination were 0.98, -0.37 and 0.65, indicating that the oxygen had a negative effect on the chlorination rate of MgO. This result was expected and agrees with equation (2). On the other hand for both the studied cases (Cr₂O₃ or MgO), the global order is almost equal to the algebraic sum of the partial orders : ⁿ(Cl₂+O₂) ≈ ⁿCl₂+ⁿO₂.

4.6. Determination of the apparent activation energy of reaction

4.6.1. Determination of E_a of the reaction from isothermal treatment

The apparent activation energy 'E_a' could be evaluated from Arrhenius equation:

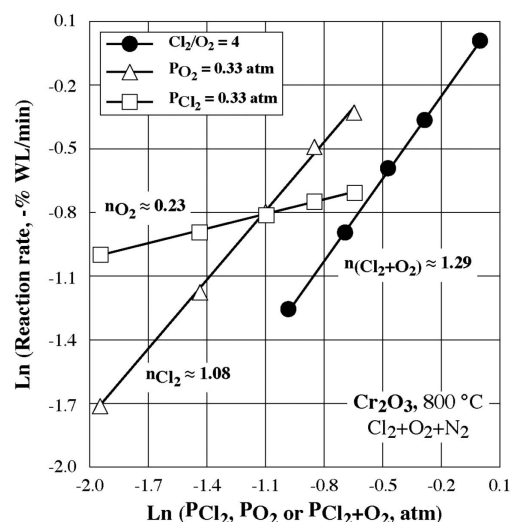


Figure 8. Evolution of the reaction rate of Cr₂O₃ oxychlorination at 800 °C versus partial pressure of reactive gases.

Figura 8. Evolución de la tasa volatilizada en la reacción de oxiclорación del Cr₂O₃ a 800 °C frente a la presión parcial de los gases reaccionantes.

$$V = k * e^{(-E_a/RT)} \quad (5)$$

or

$$\ln V = \ln K - E_a/RT \quad (6)$$

where R is the gas constant, T is the temperature in Kelvin, and k is a constant.

To determine E_a , the solid is first heated at a predetermined temperature under nitrogen atmosphere, and when a steady state is reached, the gas mixture is introduced to react with the solid at constant temperature and the evolution of the reaction extent as a function of time is recorded. Therefore, the initial reaction rate for every tested temperature is determined. The value of E_a is deduced from the slope of the straight line representing equation (6).

4.6.2. Geometry of interface (shape factor)

As the reaction of solid with chlorine takes place generally at interface of two phases, the geometry of this interface plays an important role to localize the reaction front and consequently affecting the the reaction progress. The mathematical formulations of the reaction progress (Eqs. (7) – (13)) are given for different shapes of particles. These formulations are designed as conversion functions of solid 'g(X)'. The interpretations of these functions were published by Szekely J. *et al.*^[11]. One may note that these formulations are valid when the overall reaction rate is affected by the slowest step.

Equation (7) is considered to describe a reaction controlled by the chemical reaction in the case of shrinking nonporous particles (with or without a solid porous product) and porous particles with unchanged overall size. It also applies for a mechanism affected by pore diffusion in the case of complete gasification of porous solids.

$$1-(1-X)^{1/Fp} = kt \quad (7)$$

$$X = kt \text{ for } Fp = 1 \quad (8)$$

$$1-(1-X)^{1/2} = kt \text{ for } Fp = 2 \quad (9)$$

$$1-(1-X)^{1/3} = kt \text{ for } Fp = 3 \quad (10)$$

$$X^2 = kt \text{ for } Fp = 1 \quad (11)$$

$$X+(1-X)\ln(1-X) = kt \text{ for } Fp = 2 \quad (12)$$

$$1-3(1-X)^{1/3}+2(1-X) = kt \text{ for } Fp = 3 \quad (13)$$

where

k : constant, t : reaction time,

X : extent of reaction (ratio of weight of the reacted fraction to initial weight),

Fp : particle shape factor (1, 2, and 3 for infinite slabs, long cylinders, and for spheres).

Equations (11) through (13) are pertinent to pore diffusion control in reaction of porous solids or in nonporous solids with formation of a porous solid product.

The geometry of the solid particles combined with the value of the apparent activation energy permit to suggest the rate-controlling step of the chlorine-solid reactions. The following paragraphs describe several examples.

Figure 9 groups the data obtained during the isothermal carbochlorination of Cr_2O_3 between 500 and 900 °C^[2]. The apparent activation energy is 100 ± 2 kJ/mol (Fig. 9 a)). This value tends to indicate that the overall rate of Cr_2O_3 carbochlorination in $\text{Cl}_2 + \text{CO}$ is controlled by the chemical reaction. To check this hypothesis, the mathematical formulation of the experimental data was attempted using equations (7) through (13). The best result (Fig. 9 b) and c)) of data linearization, with a correlation coefficient of ≈ 0.998 ^[10], was obtained using equation (10). This supports the hypothesis that the carbochlorination reaction of Cr_2O_3 particles is controlled by a chemical reaction according to the shrinking sphere model described by equation (10).

4.7. Chlorination kinetics of combined oxides

The oxychlorination kinetics of chromite could be presented as a case study. The chromite presents a spinel structure including Cr, Fe, Mg, and Al oxides. As mentioned in section 3, the chromite sample used had the following composition: ($\text{Fe}_{0.30}^{2+}$, $\text{Mg}_{0.70}$) ($\text{Cr}_{1.56}$, $\text{Al}_{0.37}$, $\text{Fe}_{0.07}^{3+}$) O_4 . This solid can also be formulated as: 30.9 % FeCr_2O_4 , 51.0 % MgCr_2O_4 , 13.7 % MgAl_2O_4 , and 4.4 % Fe_3O_4 . The temperature effect on the oxychlorination of chromite was explored between 600 and 1,050 °C^[2 y 6]. Results showed that the iron associated to chromium reacted with $\text{Cl}_2 + \text{O}_2$ starting at 600 °C. This reaction could be considered as that of the simple spinel FeCr_2O_4 , while MgCr_2O_4 reacts at temperature higher than 900 °C and MgAl_2O_4 seems to be refractory to the oxychlorinating gas mixture up to 1,050 °C. Figure 10 a) represents the evolution of % weight change *versus* time of the chromite sample during its reaction with $\text{Cl}_2 + \text{O}_2$ between 925 and 1,050 °C. This figure

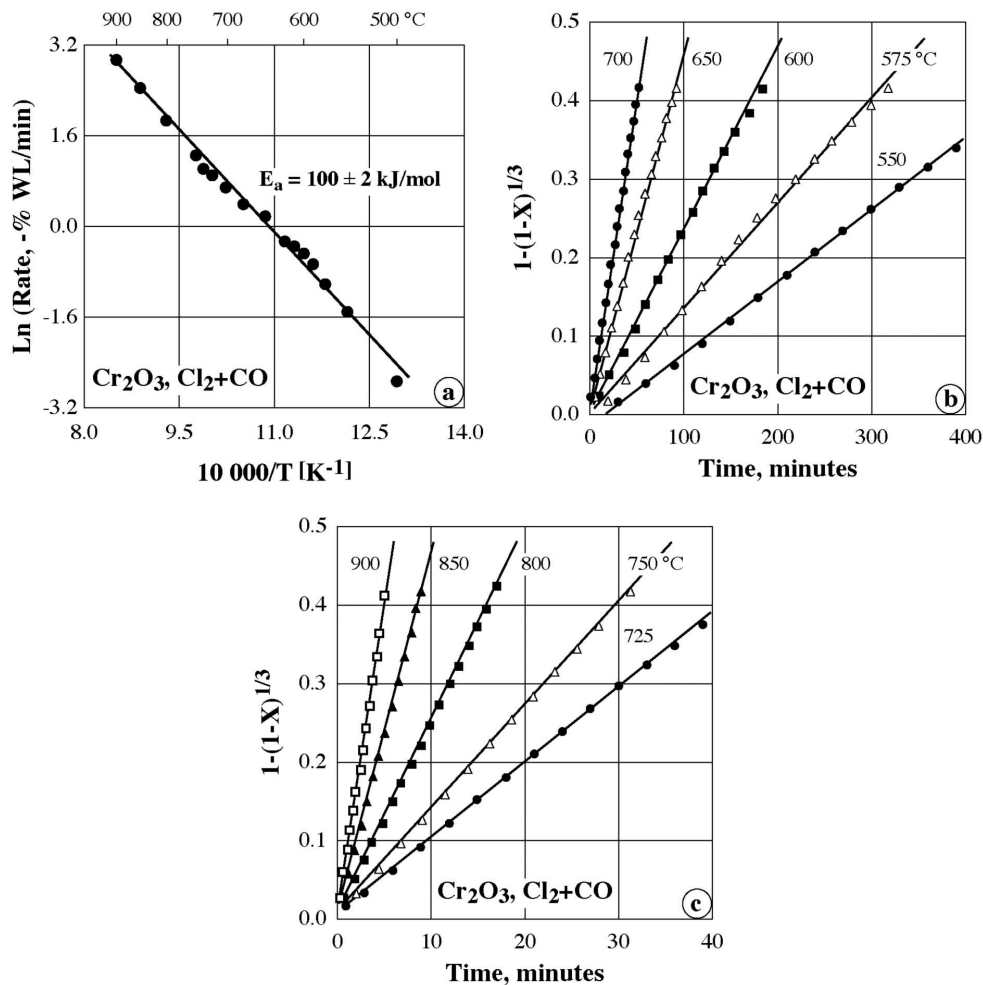


Figure 9. Plots of data obtained during isothermal carbochlorination of Cr_2O_3 in Cl_2+CO : (a) Arrhenius diagram of carbochlorination and (b) and (c) Mathematical fitting of the experimental data using equation (10).

Figura 9. Gráficos de los datos obtenidos durante la carbochloración isoterma del Cr_2O_3 en Cl_2+CO : (a) Diagrama de Arrhenius de carbochloración y (b) y (c) Ajustes matemáticos de los datos experimentales usando la ecuación (10).

shows the sharp change of the reaction rate of chromite at $X \approx 0.35$. The first part of the weight loss corresponds essentially to the chlorination of $\text{FeCr}_2\text{O}_4+\text{Fe}_3\text{O}_4$ (L^{Ch}) while the second part represents the reaction of MgCr_2O_4 with Cl_2+O_2 .

The temperature coefficient of the reaction was determined using the Arrhenius formula. It was interesting to follow the evolution of apparent activation energy as a function of reaction extent. The variation of E_a values versus the reaction extent is shown in figure 10 b) for the temperatures range of 925 to 1050 °C.

Figure 10 b) shows that the value of E_a , for X comprising between 0.05 and 0.30, is lower than 60 kJ/mol. This is followed by a sharp increase of the apparent activation energy to 260 kJ/mol for $X > 0.3$.

To get an insight of the reactions of chromite with Cl_2+O_2 , a detailed study of the effects of temperature and partial pressures of gases [$^n(\text{Cl}_2+\text{O}_2) \approx ^n\text{Cl}_2+^n\text{O}_2$] on the oxychlorination of chromite and its simple oxides (Cr_2O_3 , Fe_2O_3 , and MgO) was performed. Results are summarized in figure 11 and in table I.

Although simple oxides are included in the spinel structure of chromite, the following hypothesis can be made:

- to chlorinate the chromite constituents ($\text{FeO}.\text{Cr}_2\text{O}_3$ and/or $\text{MgO}.\text{Cr}_2\text{O}_3$) their individual oxides have to react with the chlorinating gas mixture,
- the global chlorination rate of chromite constituents depends of the slowest reaction rate of the individual oxide,

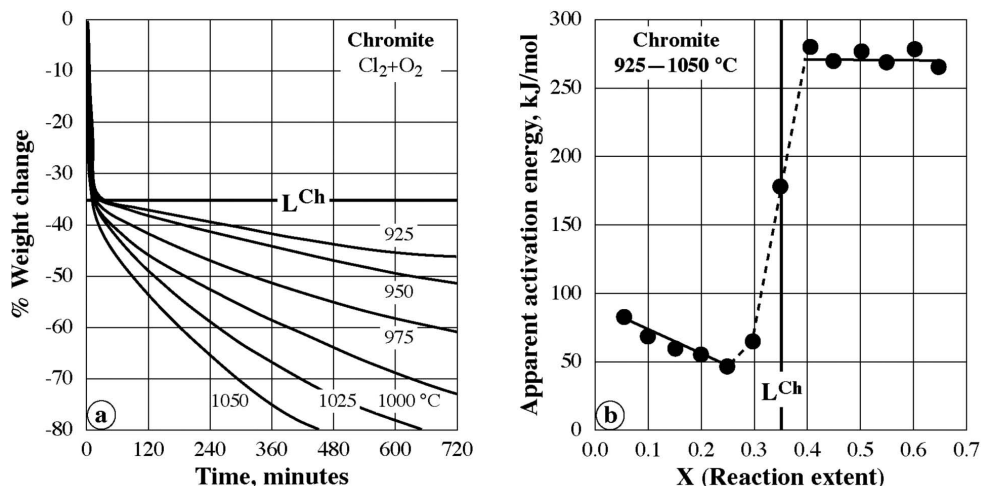


Figure 10. Oxychlorination of chromite between 925 and 1050 °C in Cl_2+O_2 atmosphere. (b) Shows the evolution of the apparent activation energy values as a function of the reaction extent calculated from the data of (a).

Figura 10. Evolución del % de cambio de peso frente al tiempo de la oxiclорación de la cromita por atmósferas de Cl_2+O_2 . La figura (b) indica la evolución de los valores de la energía aparente de activación en función de la extensión de la reacción que se puede calcular a partir de los datos expresados en la figura (a).

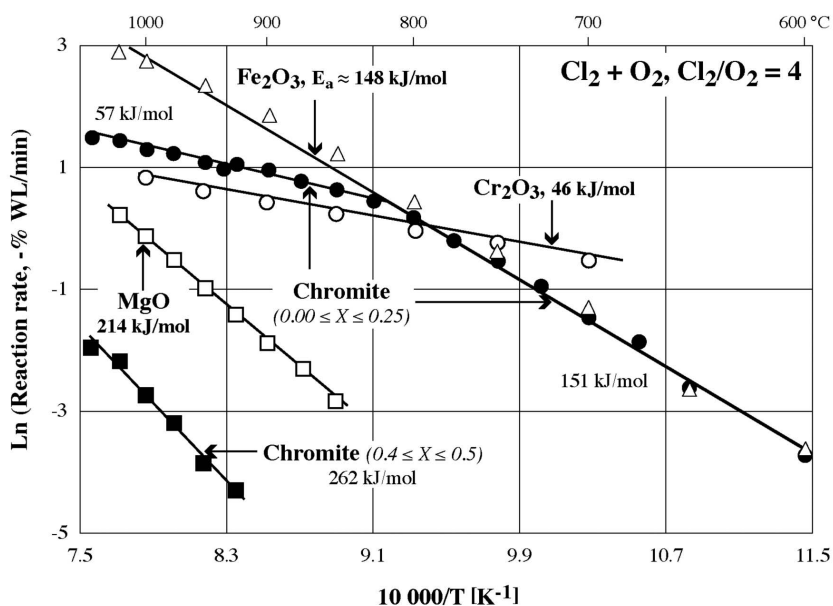


Figure 11. Arrhenius diagrams for the oxychlorination of chromite and its simple oxides in Cl_2+O_2 .

Figura 11.- Diagramas de Arrhenius de la oxiclорación de cromita y sus óxidos sencillos asociados en atmósfera. de Cl_2+O_2 .

— the kinetics parameters of the chlorination of chromite constituents should have comparable values to those of chlorination of individual oxide having the slowest reaction rate.

Figure 11 shows that the oxychlorination of chromite for $X \leq 0.25$ ($FeCr_2O_4$) is characterized by a value of $E_a \approx 151$ kJ/mol between 600 and 825 °C. A similar value is obtained for the oxychlorination of Fe_2O_3

Table I. Comparison of reaction orders with respect to reactive gases of solids' oxychlorination.

Tabla I. Comparación de los órdenes de reacción respecto de los gases reactivos de oxiclорación de sólidos.

Solids	T, °C	$n(\text{Cl}_2+\text{O}_2)$	$n\text{Cl}_2$	$n\text{O}_2$	
Cr_2O_3	800	1.29	1.08	0.23	
Fe_2O_3	750	0.71	1.44	-0.61	
	950	0.70	1.39	-0.62	
MgO	950	0.65	0.98	-0.37	
Chromite ($0.0 \leq X \leq 0.25$)	750	$(0.0 \leq X \leq 0.1)$	0.94	1.24	-0.30
		$(0.2 \leq X \leq 0.3)$	1.04	1.21	-0.24
	1000	$(0.4 \leq X \leq 0.5)$	1.23	1.03	0.16
			0.43	0.64	-0.25

($E_a \approx 148$ kJ/mol). Moreover, the oxychlorination rates of FeCr_2O_4 and Fe_2O_3 are identical. In addition, the apparent reaction orders with respect to Cl_2+O_2 , Cl_2 , and O_2 for the oxychlorination of chromite and Fe_2O_3 have the same tendency (Table I). While the kinetics parameters of Cr_2O_3 oxychlorination are different from those obtained for the chromite (Fig. 11 & Table I). These experimental results indicate that the oxychlorination rate of iron oxides governs the global rate of the FeCr_2O_4 reaction with Cl_2+O_2 for temperatures lower than 825°C .

At temperature higher than 825°C , the oxychlorination of chromite ($X \leq 0.25$) proceeds with a value of $E_a \approx 57$ kJ/mol. This value and the reaction rate are fairly similar to those obtained for Cr_2O_3 oxychlorination ($E_a \approx 46$ kJ/mol). The positive value of $n\text{O}_2$ for a determined reaction extent (Table I) reinforces the hypothesis that the oxychlorination rate of chromite ($X \leq 0.30$), at $T > 825^\circ\text{C}$ is controlled, fully or partly, by the oxychlorination rate of Cr_2O_3 .

The temperature coefficient of the chromite chlorination for $X > 0.4$ ($\text{MgO}.\text{Cr}_2\text{O}_3$) is about 262 kJ/mol from 925 to 1050°C . On the other hand, the values of E_a for Cr_2O_3 ($E_a \approx 46$ kJ/mol) and MgO ($E_a \approx 214$ kJ/mol) oxychlorination as well as those of the apparent reaction orders (Table I) suggest that the oxychlorination rate of MgO controls the global rate of chromite oxychlorination for $X \geq 0.4$ at $925\text{-}1,050^\circ\text{C}$.

This study shows that the oxychlorination of chromite proceeds in two stages characterized by different reactivities of chromite towards Cl_2+O_2 gaseous mixture. The first stage is the FeCr_2O_4

chlorination and the second one is that of MgCr_2O_4 chlorination. In both cases, the global reaction rate was affected by the slowest rate of oxychlorination of individual oxides (Fe_2O_3 , Cr_2O_3 , MgO). However, one should take into account the bond energy of simple constituents of chromite to confirm the above mentioned mechanism.

4.8. Comparison of the E_a derived from isothermal and non-isothermal conditions

The following paragraphs describe the theoretical approach^[12] for the determination of the activation energy of a gas-solid reaction from a single TGA using linear temperature rise (LTR).

The reaction rate of a gas-solid reaction could be expressed according to equation (14):

$$dX/dt = kf_1(p_A)f_2(X)f_3(d) \quad (14)$$

where X is the reaction extent, p_A is the partial pressure of the reactive gas(es) and d is the mean particle size.

The effects of partial pressure of the reactive gases, reaction extent and particle size on the reaction rate are described by $f_1(p_A)$, $f_2(X)$ and $f_3(d)$, respectively.

The temperature effect on the reaction rate is given by Arrhenius law (equation (15), using the rate constant k):

$$k = k_0 \exp(-E_a/RT) \quad (15)$$

Integration of Eq. 14 in isothermal conditions gives:

$$\int_0^X dX/f_2(X) \equiv g(X) = \int_0^t k f_1(p_A) f_3(d) dt \quad (16)$$

The conversion function of the solid $g(X)$ depends generally on the geometric change occurring in the solid as the reaction proceeds. The different types of $g(X)$ were summarized in equations (7)-(13).

If the temperature is raised linearly with respect to time the temperature evolution may be given by equation (17):

$$T = \Phi t \quad (17)$$

or

$$dT = \Phi dt \quad (18)$$

Substituting equations (15) and (17) in equation (14) and rearranging the resulting equation, it was obtained:

$$\ln[(dX/dT)g'(X)] = \ln [k_0 f_1(p_A) f_3(d)/\Phi] - E_a/RT \quad (19)$$

In the above equation, $g'(X)$ is the derivative of $g(X)$ with respect to X . The activation energy can be determined from the slope of data fitted by equation (19) when the appropriate type of $g(X)$ is determined.

4.8.1. Example of the E_a evaluation from one TGA test using LTR.

The determination of the temperature effect on the reaction of MgO with the gas mixture of $\text{Cl}_2 + \text{O}_2$ ($\text{Cl}_2/\text{O}_2 = 4$) is chosen as example. As the reactivity of MgO towards oxychlorinating gas mixture was relatively low^[2,9 y 10] the heating rate of the sample was about 1 °C/min. Figure 12 represents the obtained results concerning the oxychlorination of MgO from 575 to 1,025 °C. Magnesium oxide started to react with the oxychlorinating gas mixture at temperatures higher than 800 °C and about 70 % of the sample had reacted at 1,025 °C.

The oxychlorination reaction of MgO with $\text{Cl}_2 + \text{O}_2$ ($\text{Cl}_2/\text{O}_2 = 4$) was also studied in isothermal conditions between 850 and 1,025 °C^[8-10] in order to compare the results with those obtained using LTR method. Figure 13 traces the evolution of % weight change of the sample as a function of time during isothermal oxychlorination of MgO. The evolution of the reaction extent ($X \leq 0.7$) as function of time for all isotherms was appropriately described by equation (9)^[8 y 19]. Figure 14 a) represents the Arrhenius diagram giving the evolution of the natural logarithm of the rate constant “k” as a function of

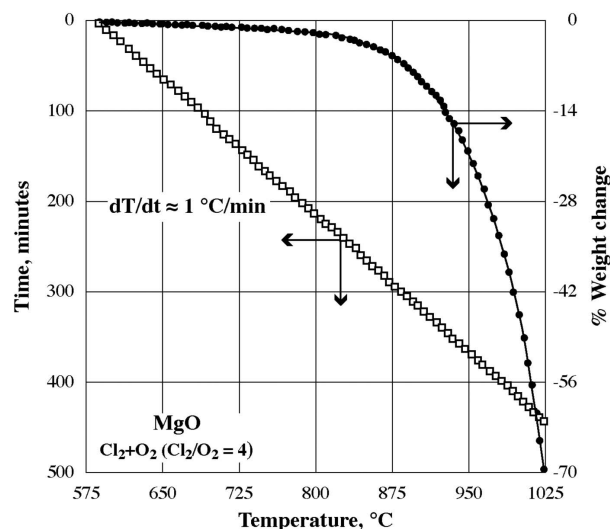


Figure 12. TGA of MgO oxychlorination using linear temperature raise.

Figura 12. Análisis termogravimétrico, ATG, de la oxiclорación utilizando un aumento lineal de la temperatura.

the inverse of temperature. A value of E_a about 213 kJ/mol was deduced from the isothermal treatment of MgO in $\text{Cl}_2 + \text{O}_2$.

Using equation (19), it is clear that the activation energy could be determined only after finding the appropriate form of $g(X)$. As for the isothermal tests, different models of the conversion function $g(X)$ were tried and the best non-isothermal data fitting was obtained by using equation (9). The data were plotted in figure 14 b) using equation (19) for $X \leq 0.70$. A value of $E_a \approx 215$ kJ/mol was deduced for the non-isothermal oxychlorination of MgO between 850 °C and 1,025 °C. Figure 14 indicates that the activation energy values calculated using the two sets of data are almost identical. These results confirm the utility of non-isothermal measurements using LTR to determine the activation energy of gas-solid reactions.

5. CONCLUSIONS

The following general conclusions can be drawn from the kinetics studies of chlorination reactions of different materials through thermo-gravimetric measurements.

- The reactivity of different solids towards chlorinating gases varied widely e.g. the reaction Cl_2 with CuFeS_2 started at room

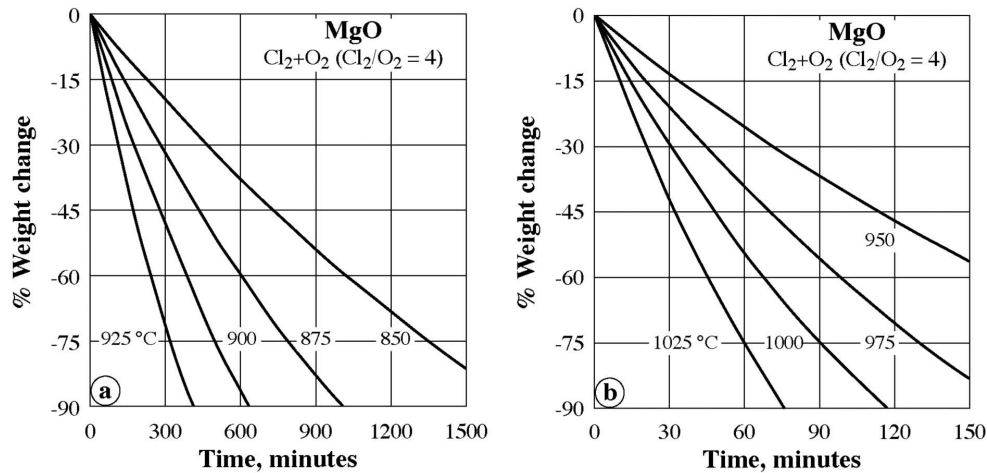


Figure 13. Evolution of the % weight change as a function of the reaction time during isothermal oxychlorination of MgO oxychlorination for (a) 850-925 °C and (b) 950-1,025 °C.

Figura 13. Evolución del cambio de peso como función del tiempo de reacción durante una oxiclora-ción isotérmica del MgO, para (a) en el intervalo 850-925 °C y (b) en el intervalo 950-1.025 °C.

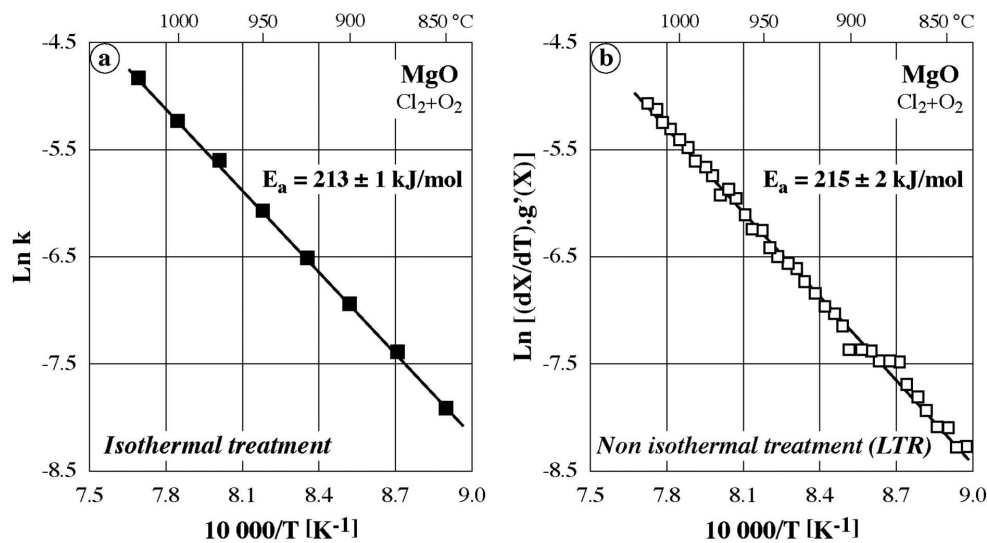


Figure 14. Arrhenius diagram of the MgO oxychlorination by Cl₂+O₂ for: (a) isothermal treatment and (b) non isothermal treatment.

Figura 14. Diagrama de Arrhenius de la oxiclora-ción del MgO en atmósfera de Cl₂+O₂, para: (a) tra-tamiento isotérmico y (b) para tratamiento no isotérmico.

temperature while carbochlorination of Cr₂O₃ required a temperature ≥ 500 °C.

- The effect of external mass and heat transfer on the reaction rate could be minimized by choosing adequate gas velocities.
- The apparent reaction orders with respect to reactive gases (Cl₂, O₂, CO), obtained experimentally, were fractions, either positive

or negative numbers. Although they differ from stoichiometric coefficients of the reaction, their positive or negative value depends on the considered chemical reactions. The apparent reaction order with respect to O₂ is 0.23 for Cr₂O₃ oxychlorination, while that of MgO oxychlorination $n_{O_2} \approx -0.37$. The oxychlorination reactions of MgO and Cr₂O₃

with Cl_2+O_2 explain this difference concerning the oxygen role in the two reactions.

- The value of E_a depends on the type of solid, the nature of the chlorinating gas mixture (Cl_2 , Cl_2+O_2 , Cl_2+CO), the studied temperature range, the physical state of the reaction products, etc
- The isothermal and the linear temperature raise techniques gave essentially similar kinetic parameters. Further, from the formulation of the reaction interface geometry, the rate controlling step could be predicted accurately.

This study thus demonstrated that, simple thermogravimetric measurements can be utilized for measurement of complex reaction kinetics involving gas – solid reactions such as chlorination of variety of solid samples with number of reactive gases compositions. The obtained kinetics information can be used for process optimization involving beneficiation of lean ores and extraction of several valuable metals from their oxide or sulfide ores, which are otherwise difficult by traditional chemical beneficiation and/or extraction methods.

REFERENCES

- [1] *Proc. 32nd Ann. Hydrometallurgy Meet. and Int. Conf. Practice and Theory of Chloride/Metal Interaction. Vol. I and II.* Eds. E. Peek and G. van Weert, Pub. Canadian Institute of Mining, Metallurgy and Petroleum, Montreal, Canada, 2002.
- [2] N. Kanari, Ph.D. Thesis, Institut National Polytechnique de Lorraine, France. 1995.
- [3] N. Kanari, E. Allain, N. Menad and I. Gaballah, *Metall Mater Trans B* 30B (1999) 567-576.
- [4] N. Kanari, I. Gaballah and E. Allain, *Thermochim. Acta* 373 (2001) 75-93.
- [5] N. Kanari, E. Allain and I. Gaballah, *Metall. Mater. Trans. B* 30 (1999) 577-587.
- [6] N. Kanari, I. Gaballah and E. Allain, *Thermochim. Acta* 371 (2001) 143-154.
- [7] N. Kanari, I. Gaballah and E. Allain, *Thermochim. Acta* 371 (2001) 75-86.
- [8] N. Kanari, I. Gaballah and E. Allain, *Metall. Mater. Trans. B* 30 (1999) 1009-1015.
- [9] N. Kanari, E. Allain and I. Gaballah, *Thermochim. Acta* 351 (2000) 131-137.
- [10] N. Kanari, Habilitation Diploma, Institut National Polytechnique de Lorraine, France, 2000.
- [11] J. Szekely, J. W. Evans and H. Y. Sohn, *Gas-Solid Reactions*, Academic Press, New York, USA, 1976, pp. 68-70, 73-88, 109-131 and 232-235.
- [12] P.C. Chaubal and H.Y. Sohn, *Metall. Mater. Trans. B* 17 (1986) 51-60.